

Magnetic-Field-Induced Antiferromagnetism in Two-Dimensional Hubbard Model: Analysis of CeRhIn₅

Keitaro SAKURAZAWA¹, Hiroshi KONTANI² and Tetsuro SASO¹

¹*Department of Physics, Saitama University, 255 Shimo-Okubo, Saitama 338-8570, Japan.*

²*Department of Physics, Nagoya University, Furo-cho, Nagoya 464-8602, Japan.*

(March 10, 2021)

We propose the mechanism for the magnetic-field-induced antiferromagnetic (AFM) state in a two-dimensional Hubbard model in the vicinity of the AFM quantum critical point (QCP), using the fluctuation-exchange (FLEX) approximation by taking the Zeeman energy due to the magnetic field \mathbf{B} into account. In the vicinity of the QCP, we find that the AFM correlation perpendicular to \mathbf{B} is enhanced, whereas that parallel to \mathbf{B} is reduced. This fact means that the finite magnetic field increases T_N , with the AFM order perpendicular to \mathbf{B} . The increment in T_N can be understood in terms of the reduction of both quantum and thermal fluctuations due to the magnetic field, which is caused by the self-energy effect within the FLEX approximation. The present study naturally explains the increment in T_N in CeRhIn₅ under the magnetic field found recently.

KEY WORDS: field-induced magnetism, FLEX, antiferromagnetic fluctuations, CeRhIn₅

Recently, critical phenomena in the vicinity of the magnetic quantum critical point (QCP) have attracted much interest in strongly correlated metals. Experimentally, the outer magnetic field is frequently used to change the distance from the QCP. As for the antiferromagnetic (AFM) QCP, the magnetic field is believed to increase the distance to the QCP in general. Spin fluctuation theories such as the SCR theory [1] and the fluctuation-exchange (FLEX) approximation [2], have succeeded in describing various critical phenomena in metals close to the AFM-QCP, such as the non-Fermi liquid-like behaviors of various transport coefficients [3,4]. However, previous studies on the effect of the magnetic field based on the spin fluctuation theory were not comprehensive [5,6].

CeMIn₅ (M=Rh, Co, or Ir) is a well-known quasi-two-dimensional heavy fermion compound, where single conductive CeIn layers stack perpendicular to the c -axis. CeCoIn₅ is a superconductor with $T_c = 2.3$ K at ambient pressure [7]. In CeRhIn₅, the AFM order emerges at $T_N = 3.8$ K at ambient pressure, and the superconductivity emerges at $T_c \approx 2$ K below $P = 1.6$ GPa [8,9]. Recent experiments reveals that the T_N *increases* under the magnetic field along the $a(b)$ -axis. When $B = 9$ T, the increment in T_N is approximately 0.15 K. A small increment in T_N is also observed in Ce₂RhIn₈ which is composed of double CeIn layers. However, there has been no theoretical explanation for this phenomenon.

In the present study, we investigate the two-dimensional Hubbard model under the uniform magnetic field \mathbf{B} along the x -axis, based on the FLEX approximation. In the vicinity of the AFM-QCP, we find that the AFM spin correlation of the $y(z)$ -component is *enhanced* by the applied magnetic field. In the obtained phase diagram, the magnetic transition temperature T_N , below which the staggered magnetism emerges on the yz -plane, increases with magnetic field. The mechanism of the field-induced antiferromagnetism (FI-AFM) proposed in the present study will be universal in low-dimensional metals close to the AFM-QCP, contrary to the fact that

the magnetic field suppresses T_N in usual models by the mean-field approximation. The present study naturally explains the enhancement in T_N under the magnetic field in CeRhIn₅.

We analyze the following two-dimensional Hubbard model:

$$H = \sum_{\mathbf{k}\sigma} \epsilon_{\mathbf{k}\sigma} c_{\mathbf{k}\sigma}^\dagger c_{\mathbf{k}\sigma} + U \sum_{\mathbf{k}\mathbf{k}'\mathbf{q}} c_{\mathbf{k}+\mathbf{q}\uparrow}^\dagger c_{\mathbf{k}'-\mathbf{q}\downarrow}^\dagger c_{\mathbf{k}'\downarrow} c_{\mathbf{k}\uparrow}, \quad (1)$$

where $\sigma = 1(-1)$ corresponds to the $\uparrow(-\downarrow)$ spin state and $\epsilon_{\mathbf{k}\sigma} = \epsilon_{\mathbf{k}} + \sigma B$, where the factor σB represents the Zeeman energy. The spin quantization axis is the x -axis. We study the square lattice tight-binding model with nearest neighbor hopping (t) and next-nearest neighbor hopping (t'). The dispersion of the electron is given by $\epsilon_{\mathbf{k}} = -2t(\cos k_x + \cos k_y) - 4t' \cos k_x \cos k_y$. We study the case of $(t, t') = (1, -0.25)$ with the electron density $n = 0.90$ ($n = 1.20$) per site, which corresponds to a hole-doped (electron-doped) high- T_c cuprates. In the case of $n = 0.90$, the Fermi surface (FS) is very close to the van-Hove singular point (at $(\pi, 0)$ in this case; see Fig. 3), and it is similar to the largest (main) cylindrical FS in CeMIn₅ (M=Co, Ir, Rh) [10]. Assuming a similar single cylindrical FS, many aspects of CeMIn₅, particularly the $d_{x^2-y^2}$ -wave superconductivity, can be reproduced by the perturbation study [11,12].

In the presence of the magnetic field along the x -axis, the dynamical spin susceptibilities within the FLEX approximation (or random-phase approximation (RPA)), $\chi_x^s(q)$ and $\chi_{y(z)}^s(q)$, are given by

$$\chi_y(q) = \chi_z(q) = (\chi_{\uparrow, \downarrow}(q) + \chi_{\downarrow, \uparrow}(q)) / 4 \quad (2)$$

$$\chi_x(q) = [\chi_{\uparrow, \uparrow}(q) + \chi_{\downarrow, \downarrow}(q)] / 4 + U \chi_{\uparrow, \uparrow}(q) \chi_{\downarrow, \downarrow}^0(q) / 2, \quad (3)$$

$$\chi_{\sigma, -\sigma}(q) = \frac{\chi_{\sigma, -\sigma}^0(q)}{1 - U \chi_{\sigma, -\sigma}^0(q)}, \quad (4)$$

$$\chi_{\sigma, \sigma}(q) = \frac{\chi_{\sigma, \sigma}^0(q)}{1 - U^2 \chi_{\sigma, \sigma}^0(q) \chi_{-\sigma, -\sigma}^0(q)}, \quad (5)$$

$$\chi_{\sigma,\sigma'}^0(q) = -T \sum_k G_\sigma(k+q)G_{\sigma'}(k). \quad (6)$$

Note that $\chi_{\uparrow,\downarrow}(q) = \{\chi_{\downarrow,\uparrow}(q)\}^*$. Here and hereafter, we promise that $q \equiv (\mathbf{q}, i\omega_n) = (\mathbf{q}, 2\pi inT)$ and $k \equiv (\mathbf{k}, i\epsilon_n) = (\mathbf{k}, \pi i(2n+1)T)$. Apparently, both $\chi_x(q)$ and $\chi_{y(z)}(q)$ are even functions of B , reflecting the reflectional symmetry in spin space. Apparently, $\chi_x(q) = \chi_y(q)$ when $B = 0$.

The self-energy in the FLEX approximation is given by

$$\begin{aligned} \Sigma_\sigma(k) = U^2 T \sum_q [G_\sigma(k-q)(\chi_{-\sigma,-\sigma}(q) - \chi_{-\sigma,-\sigma}^0(q)) \\ + G_{-\sigma}(k-q)\chi_{\sigma,-\sigma}(q)] + Un_{-\sigma}, \end{aligned} \quad (7)$$

where $n_\sigma = T \sum_k \text{Im}G_\sigma(k)e^{-i\epsilon_n \cdot 0^+}/\pi$ is the density of electrons with σ -spin. Here, we solve the Eqs. (2)-(7) together with the Dyson equation $G_\sigma^{-1}(k) = i\epsilon_n + \mu - \epsilon_{\mathbf{k}} - \sigma B - \Sigma_\sigma(k)$ numerically, by adjusting the chemical potential μ so that $n = \sum_\sigma n_\sigma$.

Here, we discuss the numerical results obtained by the FLEX approximation. We use 64×64 \mathbf{k} -meshes and 1028 Matsubara frequencies in the present numerical study by FLEX approximation. Figure 1 shows the obtained static staggered spin susceptibilities: $\chi_\alpha^{\max} \equiv \max_{\mathbf{q}} \chi_\alpha(\mathbf{q}, 0)$, where $\alpha = x, y, z$. $\alpha_S \equiv \max_{\mathbf{q}} U\chi^0(\mathbf{q}, 0)$ is the Stoner factor without B . In the FLEX approximation, $\alpha_S < 1$ is always satisfied at finite T in two-dimensional systems, so the Marmin-Wagner-Hohenberg theorem is satisfied [13,14]. The momentum dependence of $\chi_\alpha(\mathbf{q}, 0)$ ($\alpha = x, z$) and the splitting of the FS under the magnetic field are given in figs.2 and 3, respectively, in the case of $n = 0.90$.

In Fig. 1, χ_x^{\max} decreases whereas χ_y^{\max} increases with $\mathbf{B} \parallel \hat{x}$ in both cases of $n = 0.90$ and $n = 1.20$ by FLEX approximation. Their field dependence becomes more prominent as U increases, that is, as α_S approaches unity. These results indicate that the distance to the AFM-QCP decreases owing to the uniform magnetic field. In the FLEX approximation, the field dependence of the susceptibility is caused by (i) the change in the nesting conditions owing to the Zeeman splitting of the FS, and (ii) the self-energy effect (or mode-mode coupling effect) which represents the reduction in χ^{\max} and its Curie-Weiss-like temperature dependence owing to the spin-fluctuations. In the FLEX approximation, a large $\text{Im}\Sigma(\mathbf{k}, -i\delta)$ caused by spin fluctuations reduces the density of states (DOS) at μ , which makes $\chi^{\text{FLEX}} \gg \chi^{\text{RPA}}$. Below, we will discuss that the effect (ii), which is absent in the RPA is important to explain why $\chi_{y(z)}^{\max}$ is enhanced under the magnetic field parallel to the x -axis.

We discuss the physical reason for the field enhancement of the AFM correlation: First, the uniform magnetization induced by $\mathbf{B} \parallel \hat{x}$ will reduce the AFM correlation along the x -direction. This leads to the enhancement of χ_y^{\max} by contraries, as a result of solving the

conflict between spin-fluctuations with different components. The increase in χ_y^{\max} will be more prominent in lower dimensional systems because the reduction of T_N due to fluctuations is large in general. Note that the reduction of the staggered moment at $T = 0$ owing to the quantum fluctuations is approximately 40%(15%) in two (three) dimensional $S = 1/2$ Heisenberg model without a magnetic field.

Consistently with the above discussion, $\chi_{y(z)}^{\max}$ increases whereas χ_x^{\max} decreases under $\mathbf{B} \parallel \hat{x}$ in the present model by the FLEX approximation. We have checked that this is a universal behavior in two-dimensional systems close to the AFM-QCP, by studying various types of Hubbard model. Here, we briefly discuss the self-energy effect for susceptibilities: When $\mathbf{B} = 0$, $\chi_{\uparrow,\downarrow}^0(\mathbf{q}, 0)$ by the FLEX approximation is reduced from the RPA's value because of the reduction of the DOS, which is caused by the large $\text{Im}\Sigma$ under strong spin-fluctuations. Considering that $\Sigma(k) \approx U^2 T \sum_q \sum_{\alpha}^{x,y,z} \chi_\alpha(q)G^0(k+q)$, the change in $\chi_{\uparrow,\downarrow}^0(\mathbf{q}, 0)$ within the lowest order with respect to the self-energy is given by

$$\begin{aligned} \delta' \chi_{\uparrow,\downarrow}^0(\mathbf{q}, 0) \approx -T^2 \sum_{k,q'} G^0(k)^2 G^0(k+\mathbf{q})G^0(k+q') \\ \times 2U^2(\chi_x(q') + 2\chi_y(q')). \end{aligned} \quad (8)$$

Because it is negative, χ_y^{\max} in the FLEX approximation becomes smaller than that in RPA. Once $\mathbf{B} \parallel \hat{x}$ is applied, the reduction in $\chi_x(q')$ owing to the field-induced uniform magnetization will make $|\delta' \chi_{\uparrow,\downarrow}^0(\mathbf{Q}, 0)|$ smaller. Consequently, χ_y^{\max} increases in proportion to B^2 as long as only the self-energy effect is taken into account.

On the other hand, unphysical results are obtained by RPA, where all G 's in Eqs. (2)-(7) are replaced with G_0 's. In the case $n = 0.90$, both χ_x^{\max} and χ_y^{\max} by RPA increase with B as shown in Fig. 1, possibly reflecting the fact that the FS is close to the van-Hove singularity. On the contrary, both χ_x^{\max} and χ_y^{\max} decreases with \mathbf{B} when $n = 1.20$. Thus, results given by the RPA are not universal, depending sensitively on the shape of the FS. As a result, the self-energy effect included in the FLEX approximation is indispensable in reproducing the physically reasonable behavior of the two-dimensional nearly AFM metals (i.e., $\alpha_S \gtrsim 0.98$) under a magnetic field.

In the next stage, we study the magnetic-field dependence of the Néel temperature T_N by assuming a weak three-dimensional coupling [13,14]. To simplify the analysis, we define T_N in the presence of the magnetic field under the condition that $\max_{\mathbf{q}} U\chi_{\uparrow,\downarrow}^0(\mathbf{q}, 0) = \alpha_S^0$, where α_S^0 is a constant which is slightly smaller than unity. By putting $\alpha_S^0 = 1 - J_\perp/U \sim 0.99$ (J_\perp denotes the interlayer magnetic coupling strength), we obtained reasonable Néel temperatures of κ -(BEDT-TTF)₂X and TMTSF based on the dimer model [13,14]. Figure 4 shows the field dependence of T_N given by the FLEX approximation, for several α_S^0 's. We find that the field enhancement of the Néel temperature occurs in nearly

AFM metals in two dimensions, which has been pointed out in the present work for the first time. In Fig. 4, T_N starts to increase in proportion to B^2 , and it almost saturates at approximately $B^* \sim 0.3$ when $n = 0.90$. This result also means that the system approaches the AFM-QCP by applying a magnetic field. The increment in T_N is larger when $n = 0.90$, reflecting the closeness to the van-Hove singularity.

Here, it is notable that in the antiferromagnetic isotropic Heisenberg chain under the magnetic field along the x -axis, $\langle S_i^x S_j^x \rangle - M^2 \propto (-1)^{i-j} |i-j|^{-1/\eta} \cos(2\pi M(i-j))$ and $\langle S_i^y S_j^y \rangle \propto (-1)^{i-j} |i-j|^{-\eta}$, where η decreases from unity with the magnetic field [15]. Their field dependencies are consistent with the present study of a two-dimensional Hubbard model. In the XXZ-Heisenberg chain, an infinitely small magnetic field along the x -axis induces the staggered magnetization of the y -component in the case of $J_z < J_x$ [16,17]. In the opposite case, $J_z > J_x$, the staggered magnetization along the z -axis, which exists without the field, is enhanced by $\mathbf{B} \parallel \hat{x}$ [18]. We also point out that Fukusima and Kuramoto studied a localized electron model with interactions between quadrupole moments by a local approximation, and found the field enhancement in T_Q due to the suppression of fluctuations [19].

Note that the field-induced SDW is realized in the quasi-one dimensional metal, TMTSF, owing to the orbital motion of electrons, free from the Zeeman effect [20]. However, various characteristics of the FI-AFM in CeRhIn₅ do not coincide with that observed in TMTSF. In fact, CeRhIn₅ possesses both cylindrical and spherical FS's. They are naturally explained in terms of the Zeeman effect as discussed in the present study.

We now discuss the experimental results of CeMIn₅ in the present study. The bandwidth of the present model is ~ 10 . If we estimate the renormalized quasiparticle bandwidth of CeMIn₅ to be ~ 1000 K [21], the temperature $T = 0.02$ corresponds to ~ 2 K, which is close to T_c in CeCoIn₅ [22]. The magnetic field $B = 0.1$ in the present work corresponds to ~ 5 T for the $M = \pm 5/2$ Kramers doublet (KD), because the Zeeman energy for Ce³⁺ is $(6/7)\mu_B M H$ ($6/7$ is the g -value of Ce³⁺). Note that the renormalization factor averaged over the FS is 0.217 in the present FLEX approximation for $U = 5$ at $T = 0.02$. T_N in CeRhIn₅ continues to increase with the magnetic field parallel to the ab -plane, at least below 9 T; $T_N = 3.8$ K at 0 T, and $T_N(9T) - T_N(0T) \approx 0.15$ K [8,9]. Whereas T_N decreases monotonically when $\mathbf{B} \parallel \hat{c}$, as is observed in usual 3D heavy Fermion systems. This is naturally understood because the orbital motion of electrons, which is absent in the present study where \mathbf{B} is parallel to the 2D system, will destroy the AFM state to obtain the energy due to the Landau diamagnetism.

Furthermore, we discuss the anisotropy of $\hat{\chi}(q)$ in CeRhIn₅: The lowest KD of Ce³⁺-ion in CeRhIn₅ is $\Gamma_7^{(2)}$; $|z; \pm\rangle \equiv \beta |M_z = \pm 5/2\rangle - \alpha |M_z = \mp 3/2\rangle$ [23,24], which is approximately 70 K lower than the

second lowest KD. If we put $(\alpha, \beta) \approx (0.44, 0.9)$ [24], $\langle z; \pm | J_z | z; \pm \rangle = \pm(2.5\beta^2 - 1.5\alpha^2) \approx \pm 1.74$. On the other hand, $\langle x; \pm | J_x | x; \pm \rangle = \pm\sqrt{5}\alpha\beta \approx \pm 0.885$, where $|x; \pm\rangle \equiv (|z; +\rangle \mp |z; -\rangle)/\sqrt{2}$. Then, the anisotropy of the susceptibility of a single Ce³⁺-ion is $\chi_a/\chi_c \approx 1.74/0.885 = 1.97$, which is similar to the experimental ratio. On the other hand, several neutron experiments on CeRhIn₅ revealed that the magnetic moments on Ce sites lie on the ab -plane below T_N , whose effective moment is $\mu_{\text{eff}} = 0.264\mu_B$ [23,24]. This suggests that the antiferromagnetic RKKY interaction between nearest neighbor Ce sites is XY-like; $J_{a,b} > J_c$ [25]. Then, the magnetic field along the a -axis will enhance the AFM correlation along the b -axis as a result of the reduction of fluctuations, which is similar to the behavior of the XXZ-Heisenberg chain under \mathbf{B} [16,17]. In fact, μ_{eff} is much smaller than $(6/7)\mu_B \langle x; + | J_x | x; + \rangle \approx 0.76\mu_B$, which suggests that the quantum fluctuations are strong in CeRhIn₅, reflecting its two-dimensionality. As a result, the field-enhancement in T_N observed in CeRhIn₅ is well understood in terms of the reduction of spin-fluctuations by a magnetic field. It is a future research problem to take the Kondo effect into account beyond the FLEX approximation.

In summary, on the basis of the FLEX approximation, we found the field-induced antiferromagnetism in a two-dimensional Hubbard model, as a result of solving the conflict between fluctuation with different directions by a magnetic field. This phenomenon is expected to be prominent and universal in the vicinity of the AFM-QCP in lower dimensional systems, irrespective of the fact that the field-induced uniform magnetization tends to decrease the AFM moments. The induced AFM moments are almost on the plane perpendicular to the applied magnetic field, to earn the Zeeman energy by canting. Experimentally, the field-induced increment in T_N will be more prominent when \mathbf{B} is parallel to the 2D system, because the reduction of T_N caused by the orbital motion effect (Landau quantization) is absent.

As for two-dimensional organic metals, the field-induced transition from the paramagnetic metal to the AF insulator is found in κ -(ET)₂Cu[N(CN)₂]Cl under a pressure, below $T_{c0} = 13$ K and above H_{c2} [26]. Also, field-induced SDW due to the Zeeman effect is expected to be realized in τ -phase organic metals [27]. These phenomena will be explained by the present mechanism [28].

Finally, we note that the present results by the FLEX approximation seems reasonable in terms of the fluctuation-dissipation theorem; $\langle S_\alpha^2 \rangle = \sum_{\mathbf{q}} \int_0^\infty \frac{d\omega}{\pi} \text{Im} \chi_\alpha(q) \coth(\frac{\omega}{2T})$ ($\alpha = x, y, z$), and $\sum_{\alpha=x,y,z} \langle S_\alpha^2 \rangle \approx \frac{3n}{4}$ in strongly correlated systems. When $\chi_\alpha(Q)$ grows, $\langle S_\alpha^2 \rangle$ will increase (especially in 2D systems). Thus, $\chi_{y(z)}(Q)$ will increase when $\chi_x(Q)$ decreases by $\mathbf{B} \parallel \hat{x}$ [28].

We are grateful to K. Yamada, D.S. Hirashima, K. Miyake, Y. Kuramoto, M. Tsuchiizu and Y. Matsuda for useful discussions.

-
- [1] T. Moriya and K. Ueda: *Adv. Physics* **49** (2000) 555.
- [2] N. E. Bickers and S. R. White: *Phys. Rev. B* **43** (1991) 8044.
- [3] H. Kontani, K. Kanki and K. Ueda: *Phys. Rev. B* **59** (1999) 14723.
- [4] H. Kontani: *Phys. Rev. Lett.* **89** (2003) 237003.
- [5] Effect of the magnetic field on a model close to the ferromagnetic CQP was studied in S. Shioda, Y. Takahashi and T. Moriya: *J. Phys. Soc. Jpn.* **57** (1988) 3146.
- [6] Hatatani and K. Miyake: thesis (2001).
- [7] C. Petrovic et al.: *J. Phys.: Condens. Matter* **13** (2001) L337.
- [8] A.L. Cornelius, P.G. Pagliuso, M.F. Hundley, and J.L. Sarrao: *Phys. Rev. B* **64** (2001) 144411.
- [9] B.E. Light, R.S. Kumar, A.L. Cornelius, P.G. Pagliuso, and J.L. Sarrao: *Phys. Rev. B* **69** (2004) 024419.
- [10] T. Maehira, T. Hotta, K. Ueda and A. Hasegawa: *J. Phys. Soc. Jpn.* **72** (2003) 854.
- [11] Y. Nisikawa, H. Ikeda and K. Yamada: *J. Phys. Soc. Jpn.* **71** (2002) 1140.
- [12] Y. Yanase, T. Jujo, T. Nomura, H. Ikeda, T. Hotta and K. Yamada: *Phys. Rep.* **387** (2003) 1.
- [13] H. Kino and H. Kontani: *J. Phys. Soc. Jpn.* **67** (1998) 3691.
- [14] H. Kino and H. Kontani: *J. Phys. Soc. Jpn.* **68** (1999) 1481.
- [15] T. Hikihara and A. Furusaki: *Phys. Rev. B* **69** (2004) 064427.
- [16] J.S. Caux, F.H.L. Essler and U. Low: *Phys. Rev. B* **68** (2003) 134431.
- [17] D.V. Dmitriev and V.Y. Krivnov: *cond-mat/0403035*.
- [18] Y. Hieida, K. Okunishi and Y. Akutsu: *Phys. Rev. B* **64** (2001) 224422.
- [19] N. Fukushima and Y. Kuramoto: *J. Phys. Soc. Jpn.* **67** (1998) 2460.
- [20] T. Ishiguro, G. Saito and K. Yamaji: *Organic Superconductors* (Springer, Berlin 1990), section 9.
- [21] In the LDA study of CeMIn₅, the bandwidth of heavy-quasiparticles given by the *c-f* mixing is larger than 1000K. Here, we analyze the “renormalized band” owing to the many-body effect, using the FLEX approximation in terms of the “residual interaction”; see ref. [12].
- [22] By solving the Eliashberg equation within the FLEX approximation, $T_c \approx 0.02$ with $d_{x^2-y^2}$ -wave symmetry is obtained in the preset model.
- [23] W. Bao, P.G. Pagliuso, J.L. Sarrao, J.D. Thompson, Z. Fisk, J.W. Lynn and R.W. Erwin: *Phys. Rev. B* **62** (2000) R14621.
- [24] A.D. Christianson, J.M. Lawrence, P.G. Pagliuso, N.O. Moreno, J.L. Sarrao, J.D. Thompson, P.S. Riseborough, S. Kern, E.A. Goremychkin, and A.H. Lacerda: *Phys. Rev. B* **66** (2002) 193102.
- [25] The second lowest KD or the *l-s* coupling term in *p*-orbital may be indispensable because $J_a = J_b = J_c$ in the present crystal structure within the single KD; see

H. Shiba, K. Ueda and O. Sakai: *J. Phys. Soc. Jpn* **69** (2000) 1493; T. Takimoto: unpublished.

[26] F. Kagawa, T. Itou, K. Miyagawa, and K. Kanoda: *Phys. Rev. Lett.* **93** (2004) 127001.

[27] D. Graf, E.S. Choi, J.S. Brooks, N. Harrison, K. Murata, T. Konoike, G. Papavassilou, G.A. Mousdis: *cond-mat/0406560*.

[28] present authors: in preparation.

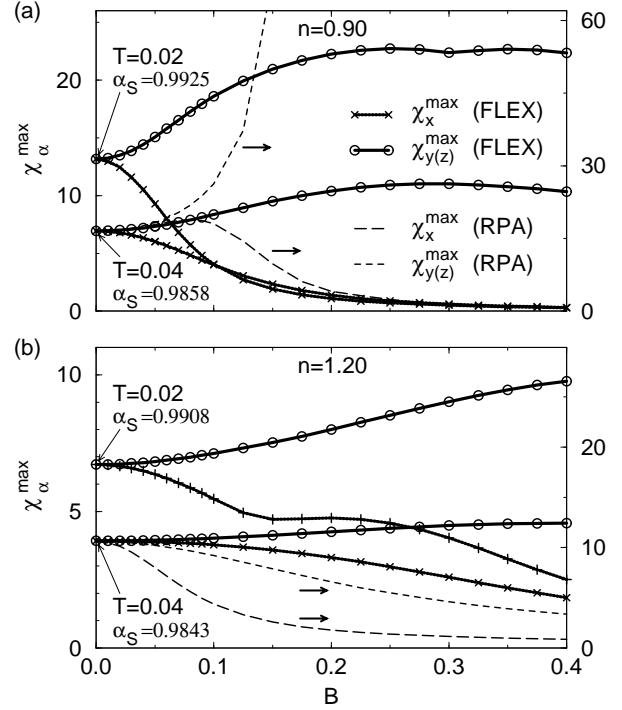


FIG. 1. Field dependences of χ_x^{\max} and χ_y^{\max} by the FLEX approximation (RPA), under conditions (a) $n = 0.90$, $U = 5$ ($U = 2.10$) and (b) $n = 1.20$, $U = 8$ ($U = 2.96$), at $T = 0.02$. In the numerical study by RPA, 256×256 *k*-meshes and 256 Matsubara frequencies are used.

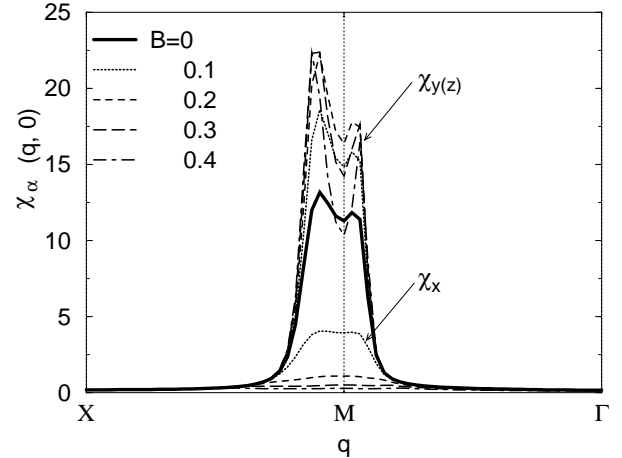


FIG. 2. $\chi_x(\mathbf{q}, 0)$ and $\chi_y(\mathbf{q}, 0)$ under finite B for $n = 0.90$ at $T = 0.02$.

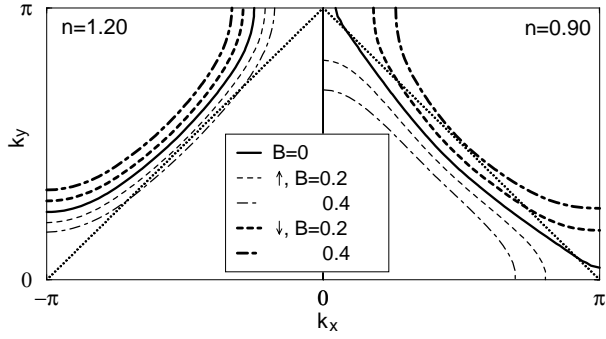


FIG. 3. FS's for \uparrow - and \downarrow -electrons under various magnetic fields for $n = 0.90$ and 1.20 at $T = 0.02$.

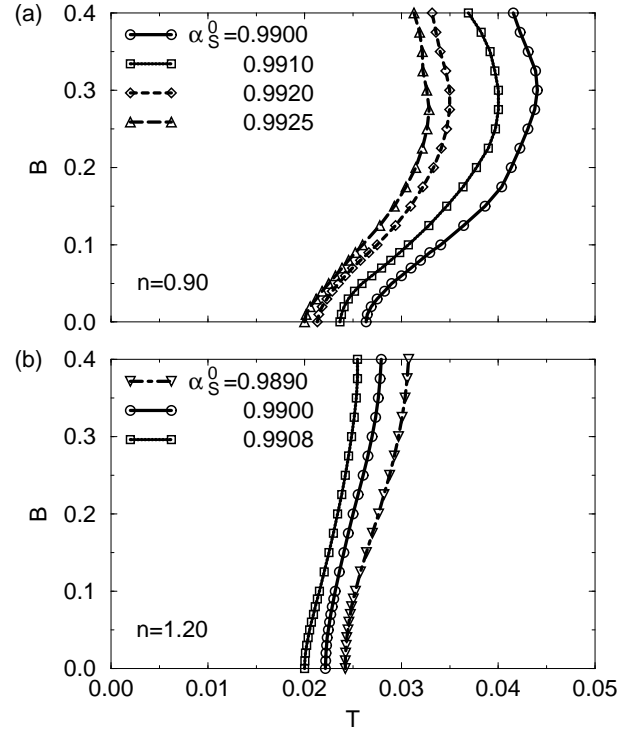


FIG. 4. Obtained phase diagram for T_N vs B for various α_S^0 's.